Weierstraß-Institut

für Angewandte Analysis und Stochastik

im Forschungsverbund Berlin e. V.

Preprint ISSN 0946 – 8633

Error control for the approximation of Allen–Cahn and Cahn–Hilliard equations with a logarithmic potential

Sören Bartels[1], Rüdiger Müller[2]

submitted: September 30, 2010

[1] Institut für Numerische Simulation
Rheinische Friedrichs-Wilhelms-Universität Bonn
Wegelerstr. 6
53115 Bonn
E-Mail: bartels@ins.uni-bonn.de

[2] Weierstraß-Institut
für Angewandte Analysis
und Stochastik
Mohrenstr. 39
10117 Berlin
E-Mail: mueller@wias-berlin.de

No. 1539
Berlin 2010

2000 *Mathematics Subject Classification.* 65M60,65M15,35K55.

Key words and phrases. Allen–Cahn equation, Cahn–Hilliard equation, logarithmic potential, finite element method, error analysis, adaptive methods.

Edited by
Weierstraß-Institut für Angewandte Analysis und Stochastik (WIAS)
Mohrenstraße 39
10117 Berlin
Germany

Fax: +49 30 2044975
E-Mail: preprint@wias-berlin.de
World Wide Web: http://www.wias-berlin.de/

ABSTRACT. A fully computable upper bound for the finite element approximation error of Allen–Cahn and Cahn–Hilliard equations with logarithmic potentials is derived. Numerical experiments show that for the sharp interface limit this bound is robust past topological changes. Modifications of the abstract results to derive quasi-optimal error estimates in different norms for lowest order finite element methods are discussed and lead to weaker conditions on the residuals under which the conditional error estimates hold.

1. Introduction

Phase separation or melting processes in multi-component alloys are often modeled as gradient flows of energy functionals of the form

$$\mathcal{E}_\gamma(u) := \frac{\gamma}{2}\int_\Omega |\nabla u|^2 \,\mathrm{d}x + \gamma^{-1}\int_\Omega F(u)\,\mathrm{d}x, \tag{1}$$

where Ω is a bounded Lipschitz domain in $\mathbb{R}^d$, $d = 2,3$, $\gamma > 0$ a small parameter, and $F : \mathbb{R} \to \mathbb{R}\cup\{+\infty\}$ a non-convex functional. For binary alloys F has a double well structure and its two minima correspond to the two phases. For temperatures θ close to the transition temperature θ_c, polynomial, e.g., quartic, growth of F provides a good description whereas for other situations, a logarithmic growth of F seems more appropriate, e.g., the functional

$$F(u) := \frac{\theta}{2}\big[(1+u)\ln(1+u) + (1-u)\ln(1-u)\big] - \frac{\theta_c}{2}u^2 \tag{2}$$

with $0 < \theta \le \theta_c$ is often employed in practice. We refer the reader to [AC79, Cah61, CH58, ES86, PF90] for details on the mathematical model and to [CE92] for a detailed discussion of the case $\theta \ll \theta_c$.

Robust error estimates, i.e., error estimates that depend on the parameter γ only in a low order polynomial, have recently been derived in [FP03, FP04, KNS04, Bar05, FW08, BM10a] for the finite element approximation of Allen–Cahn and Cahn–Hilliard equations, i.e., the L^2 and H^{-1} gradient flow of $\mathcal{E}_\gamma$, respectively, for smooth potentials F, e.g., the quartic double well potential. Those estimates are based on uniform bounds for the spectrum of the linearized Allen–Cahn or Cahn–Hilliard operator which have been derived for the smooth evolution of interfaces in [Che94, ABC94, dMS95] but fail to hold when topological changes take place. In the recent papers [BMO09, BM10b] it has been demonstrated that modifications of the techniques are possible which lead to error estimates that hold past topological changes. The key observation is that the temporal average of the principal eigenvalue of the linearized Allen–Cahn operator is bounded logarithmically past topological changes and this quantity enters error estimates exponentially. This has been formulated in terms of a conditional stability analysis and an a posteriori error analysis in which all information about the evolution are extracted from the approximate solution. Analytical evidence for the observation on the behavior of the time-averaged principal eigenvalue has been provided in [Bar10].

In this work, we aim at deriving similar estimates for Cahn–Hilliard evolutions and for the practically more relevant case of a potential with logarithmic growth such as (2). This model has first been studied numerically in [BB95] where a priori error estimates for finite element schemes where derived via a regularization of the logarithmic potential. Here, we will exploit the structure of F as the sum of a convex and a concave function. This will permit us to derive an error equation to which we may apply a generalized Gronwall lemma. The resulting error estimate holds under a condition that can be verified a posteriori and bounds the approximation error in terms of computable quantities. An analogous a priori error analysis is possible but would require an assumption owing to the lack of appropriate a priori knowledge. We also employ a reconstruction argument developed in [MN03, LM06] to derive quasi-optimal estimates in weaker norms. This is an important aspect

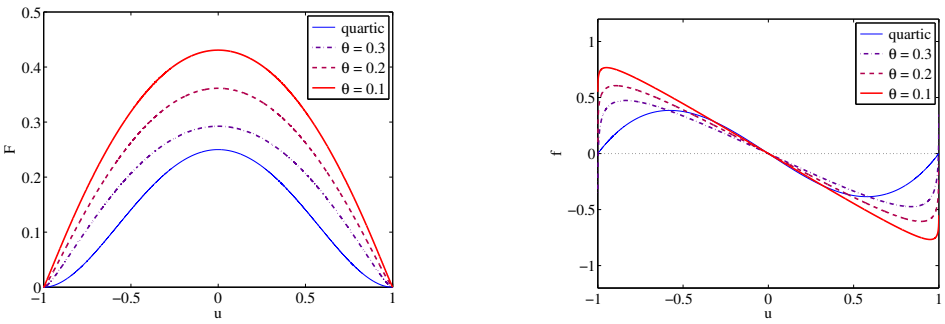

FIGURE 1. Logarithmic potential F for $\theta_c = 1$ and different temperatures θ compared to smooth quartic potential (left) and corresponding free energy density contribution $f(u) = F'(u)$ (right).

since such estimates lead to error estimates that hold under weaker conditions on the residual, cf. [BM10b].

The concept behind our results is a conditional stability result for approximate solutions of the Allen–Cahn or Cahn–Hilliard equation. Given the exact and an approximate solution u and U, respectively, we consider the principal eigenvalue of the linearized Allen–Cahn or Cahn–Hilliard operator about the approximate solution U, e.g.,

$$-\Lambda(t) = \inf_{\eta} \frac{\|\nabla\eta\|^2 + \gamma^{-2}(f'(U)\eta,\eta)}{\|\eta\|^2}$$

in the case of Allen–Cahn equations. Then, we employ a linearization of the nonlinearity in the error equation, i.e.,

$$\partial_t e - \Delta e = -\gamma^{-2} f'(U)e - \gamma^{-2}(f(u) - f(U) - f'(U)e) + r_U,$$

where r_U is the residual or discrepancy related to the approximate solution U. Splitting the first term on the right-hand side and testing the equation with e allows us to incorporate the principal eigenvalue in the error equation. We control the linearization error via

$$-(f(u) - f(U) - f'(U)e, e) \le \|\tilde{g}(U)\|_{L^\infty(\Omega)} \|e\|^3_{L^3(\Omega)}$$

and obtain

$$\begin{aligned}
\frac{1}{2}\frac{d}{dt}\|e\|^2 + \|\nabla e\|^2 &\le -\gamma^{-2}(1-\gamma^2)(f'(U)e,e) - (f'(U)e,e) + \gamma^{-2}\|\tilde{g}(U)\|_{L^\infty(\Omega)}\|e\|^3_{L^3(\Omega)} + \langle r_U, e\rangle \\
&\le (1-\gamma^2)\Lambda(t)\|e\|^2 + (1-\gamma^2)\|\nabla e\|^2 + \|f'(U)\|_{L^\infty(\Omega)}\|e\|^2 + \gamma^{-2}\|\tilde{g}(U)\|_{L^\infty(\Omega)}\|e\|^3_{L^3(\Omega)} + \langle r_U, e\rangle \\
&\le (\Lambda^+(t) + \|f'(U)\|_{L^\infty(\Omega)})\|e\|^2 + (1-\gamma^2/2)\|\nabla e\|^2 + \gamma^{-2}\|\tilde{g}(U)\|_{L^\infty(\Omega)}\|e\|^3_{L^3(\Omega)} + \frac{\gamma^{-2}}{2}\|r_U\|^2_*,
\end{aligned}$$

where $\Lambda^+(t)$ is the positive part of $\Lambda(t)$. We thus have

$$\frac{1}{2}\frac{d}{dt}\|e\|^2 + \frac{\gamma^2}{2}\|\nabla e\|^2 \le (\Lambda^+(t) + \|f'(U)\|_{L^\infty(\Omega)})\|e\|^2 + \gamma^{-2}\|\tilde{g}(U)\|_{L^\infty(\Omega)}\|e\|^3_{L^3(\Omega)} + \frac{\gamma^{-2}}{2}\|r_U\|^2_*.$$

Provided that $\|r_U\|_*$ is sufficiently small, a generalized Gronwall lemma leads to an error estimate that depends exponentially on $E = \int_0^T \Lambda^+(t)\,dt$. The smallness condition on $\|r_U\|_*$ can be formulated explicitly and involves the quantity E. This condition can not be avoided since the derived error inequality has a blowup structure. This seems to be suboptimal since solutions for Allen–Cahn equations exist globally in time.

The main contributions of this article are (i) the derivation of conditional error estimates for Cahn–Hilliard equations that are robust past topological changes, (ii) the treatment of logarithmic potentials for Allen–Cahn and Cahn–Hilliard equations, (iii) the derivation of quasi-optimal estimates in weaker norms for non-standard finite element methods, (iv) the numerical verification of the validity of the conditional a posteriori error estimate, and (v) numerical experiments that indicate partial robustness also with respect to critical transition temperatures.

We remark that our analysis also covers the case of Cahn–Hilliard equations with smooth potentials defined on $\mathbb{R}$. In this case it is necessary to assume that the exact and approximate solutions are bounded uniformly by some constant. This is however not a restrictive condition as the estimates of [CM95] show. Alternatively, one may impose certain growth conditions on f and argue as in [BM10a].

Various other important aspects of the numerical analysis of phase field models such as concentration dependent or degenerate mobilities, convergence to the sharp interface model, or singular potentials as limits for $\theta \to 0$ leading to double obstacle problems are not covered in this article and the reader is referred to [BE91, BE92, EG96, NV97, BB99, BBG99, BN09].

The outline of our paper is as follows. In Section 2 we will discuss some elementary facts about the logarithmic free energy and specify our notation. Abstract error estimates for Allen–Cahn and Cahn–Hilliard models with logarithmic free energy are derived in Sections 3 and 4, respectively. A discussion of the derivation of estimates in weaker norms is provided in Section 5. Details on the numerical treatment of the logarithmic potential and numerical experiments discussing our abstract error estimates are reported in Section 6.

2. Preliminaries

2.1. **Structure of the logarithmic potential.** Fundamental to our analysis is a splitting of F into a concave and a smooth, convex part.

Assumption (GA). *Let $0 < \theta \le \theta_c$. There exists an open interval $I \subseteq \mathbb{R}$ and functions $\psi \in C^2(I)$, $\phi \in C^4(I)$ satisfying $\phi'', \phi^{(4)} \ge 0$ in I and*

$$(\psi'(a) - \psi'(b))(a-b) \ge \psi''(a)(a-b)^2 - g(a)|a-b|^3$$

for all $a, b \in I$ with a nonnegative function $g \in C(I)$ and

$$F = \theta\phi + \theta_c\psi \quad \text{in } I.$$

Remark 2.1. *The condition $\phi'' \ge 0$ in I implies that ϕ is convex and ϕ' is monotone. A Taylor expansion and $\phi^{(4)} \ge 0$ in I show that for all $a, b \in I$ we have*

$$(\phi'(a) - \phi'(b))(a-b) \ge \phi''(a)(a-b)^2 - \phi'''(a)(a-b)^3/2.$$

Example 2.2. *For F as in (2) we have that (GA) is satisfied with $I = (-1,1)$, $\psi(u) = -u^2/2$, $\phi(u) = \big[(1+u)\ln(1+u) + (1-u)\ln(1-u)\big]/2$, and $g \equiv 0$: straightforward calculations show*

$$(\psi'(a) - \psi'(b))(a-b) = -(a-b)^2 = \psi''(a)(a-b)^2$$

for all $a, b \in I$ and

$$\phi'(u) = \frac{1}{2}\ln\Big(\frac{1+u}{1-u}\Big), \quad \phi''(u) = \frac{1}{1-u^2}, \quad \phi'''(u) = \frac{2u}{(1-u^2)^2}, \quad \phi^{(4)}(u) = \frac{2+6u^2}{(1-u^2)^3}.$$

2.2. **Generalized Gronwall lemma.** The second key ingredient is a generalized Gronwall lemma which allows an additional superlinear term.

Lemma 2.3 ([BMO09]). *Suppose that the nonnegative functions $y_1 \in C([0,T])$, $y_2, y_3 \in L^1(0,T)$, $\alpha \in L^\infty(0,T)$, and the real number $A \geq 0$ satisfy*

$$y_1(t) + \int_0^t y_2(s)\,\mathrm{d}s \leq A + \int_0^t \alpha(s) y_1(s)\,\mathrm{d}s + \int_0^t y_3(s)\,\mathrm{d}s$$

for all $t \in [0,T]$. Assume that for $B \geq 0$, $\beta > 0$, and every $t \in [0,T]$ we have

$$\int_0^t y_3(s)\,\mathrm{d}s \leq B \sup_{s\in[0,t]} y_1^\beta(s) \int_0^t (y_1(s) + y_2(s))\,\mathrm{d}s.$$

Set $E := \exp\big(\int_0^T \alpha(s)\,\mathrm{d}s\big)$ and assume that $8AE \leq (8B(1+T)E)^{-1/\beta}$. We then have

$$\sup_{t\in[0,T]} y_1(t) + \int_0^T y_2(s)\,\mathrm{d}s \leq 8A \exp\Big(\int_0^T \alpha(s)\,\mathrm{d}s\Big).$$

2.3. **Notation.** Throughout this article we employ standard notation for Sobolev spaces. The L^2 norm in Ω is abbreviated by $\|\cdot\|$ and the corresponding scalar product by $(\cdot,\cdot)$. We let $\langle\cdot,\cdot\rangle$ denote the duality pairing of a Banach space $\mathbb{V}$ and its dual $\mathbb{V}'$. The positive part of a real number s is denoted s^+, i.e., $s^+ := \max\{s,0\}$ for all $s \in \mathbb{R}$. Given a function $\eta \in L^1(\Omega)$ we let $\overline{\eta}$ denote the average of η in Ω, i.e.,

$$\overline{\eta} = \frac{1}{|\Omega|}\int_\Omega \eta\,\mathrm{d}x.$$

3. Abstract error analysis for Allen–Cahn equations

In this section we discuss an abstract error estimate for the approximation of Allen–Cahn equations with general, non-smooth potentials. Throughout this section we set

$$\mathbb{V} := H^1(\Omega)$$

and

$$X_{AC} := H^1(0,T;\mathbb{V}') \cap L^2(0,T;\mathbb{V}).$$

Moreover, we let $f = F'$ denote the derivative of F.

Definition 3.1. *a) For $\ell = 1,2$ let $u_\ell \in X_{AC}$ define the* residuals *$r_\ell \in L^2(0,T;\mathbb{V}')$ such that*

$$\langle r_\ell, \eta\rangle = \langle \partial_t u_\ell, \eta\rangle + (\nabla u_\ell, \nabla\eta) + \gamma^{-2}(f(u_\ell),\eta)$$

for all $\eta \in \mathbb{V}$ and almost everywhere in $[0,T]$. If $r_\ell = 0$ almost everywhere in $[0,T]$, we call u_ℓ a weak solution of the Allen–Cahn equation.
b) For almost every $t \in [0,T]$ let the principal eigenvalue *$-\lambda_{AC}(t)$ be defined through*

$$-\lambda_{AC}(t) := \inf_{\eta\in\mathbb{V}\setminus\{0\}} \frac{\|\nabla\eta\|^2 + \gamma^{-2}(f'(u_1(t))\eta,\eta)}{\|\eta\|^2}.$$

c) Set $e := u_1 - u_2$ and $r := r_1 - r_2$. The functions $\mu_0, \mu_1 : [0,T] \to \mathbb{R}$ are residual estimators *if*

$$\langle r(t),\eta\rangle \leq \mu_0(t)\|\eta\| + \mu_1(t)\|\nabla\eta\|$$

for almost every $t \in [0,T]$ and all $\eta \in \mathbb{V}$.

Proposition 3.2. *Let (GA) hold and assume $0<\gamma\le 1$ and that there are residual estimators according to Definition 3.1. For almost every $t\in[0,T]$ define*

$$\alpha(t) := 2\big(\theta_c\|\psi''(u_1(t))\|_{L^\infty(\Omega)} + (1-\gamma^2)\lambda_{AC}(t) + 1/2\big)^+,$$
$$B := 2\gamma^{-4}C_S^2 \sup_{s\in[0,T]} \big(2\theta_c\|g(u_1(s))\|_{L^\infty(\Omega)} + \theta\|\phi'''(u_1(s))\|_{L^\infty(\Omega)}\big)$$

and suppose that with $E := \exp\big(\int_0^T \alpha(s)\,\mathrm{d}s\big)$ we have

$$\int_0^T (\mu_0^2 + \gamma^{-2}\mu_1^2)\,\mathrm{d}s + \|e(0)\|^2 \le (8E)^{-3}B^{-2}(1+T)^{-2}.$$

Then we have

$$\sup_{s\in(0,T)} \|e(s)\|^2 + \gamma^2\int_0^T \|\nabla e\|^2\,\mathrm{d}s \le 8\Big(\int_0^T (\mu_0^2+\gamma^{-2}\mu_1^2)\,\mathrm{d}s + \|e(0)\|^2\Big)$$
$$\times \exp\Big(2\int_0^T \big(\theta_c\|\psi''(u_1(s))\|_{L^\infty(\Omega)} + (1-\gamma^2)\lambda_{AC}(s) + 1/2\big)^+\,\mathrm{d}s\Big).$$

Proof. Subtracting the equations for u_1 and u_2 and choosing $\eta = e$ we find, using the assumed estimate for ψ and the monotonicity of ϕ', that

$$\begin{aligned}\frac{1}{2}\frac{d}{dt}\|e\|^2 + \|\nabla e\|^2 &= -\gamma^{-2}(f(u_1)-f(u_2),e) + \langle r,e\rangle \\ &= -\gamma^{-2}\theta_c(\psi'(u_1)-\psi'(u_2),e) - \gamma^{-2}\theta(\phi'(u_1)-\phi'(u_2),e) + \langle r,e\rangle \\ &\le \gamma^{-2}\theta_c\|\psi''(u_1)\|_{L^\infty(\Omega)}\|e\|^2 + \gamma^{-2}\theta_c\|g(u_1)\|_{L^\infty(\Omega)}\|e\|_{L^3(\Omega)}^3 + \langle r,e\rangle.\end{aligned} \tag{3}$$

Analogously, but using that owing to (GA) and Remark 2.1 we have

$$\begin{aligned}(f(a)-f(b))(a-b) &= \theta_c(\psi'(a)-\psi'(b))(a-b) + \theta(\phi'(a)-\phi'(b))(a-b) \\ &\ge \theta_c\psi''(a)(a-b)^2 - \theta_c g(a)(a-b)^3 + \theta\phi''(a)(a-b)^2 - \theta\phi'''(a)(a-b)^3/2 \\ &= f'(a)(a-b)^2 - \theta_c g(a)(a-b)^3 - \theta\phi'''(a)(a-b)^3/2\end{aligned} \tag{4}$$

for all $a,b\in I$ and incorporating the definition of λ_{AC}, we find

$$\begin{aligned}\frac{1}{2}\frac{d}{dt}\|e\|^2 + \|\nabla e\|^2 &= -\gamma^{-2}(f(u_1)-f(u_2),e) + \langle r,e\rangle \\ &\le -\gamma^{-2}(f'(u_1)e,e) + \gamma^{-2}\big(\theta_c|g(u_1)\|_{L^\infty(\Omega)} + \theta\|\phi'''(u_1)\|_{L^\infty(\Omega)}\big)\|e\|_{L^3(\Omega)}^3 + \langle r,e\rangle \\ &\le \lambda_{AC}\|e\|^2 + \|\nabla e\|^2 + \gamma^{-2}\big(\theta_c\|g(u_1)\|_{L^\infty(\Omega)} + \theta\|\phi'''(u_1)\|_{L^\infty(\Omega)}\big)\|e\|_{L^3(\Omega)}^3 + \langle r,e\rangle.\end{aligned} \tag{5}$$

We multiply (3) by γ^2 and (5) by $(1-\gamma^2)$ and add the resulting estimates to deduce that

$$\begin{aligned}\frac{1}{2}\frac{d}{dt}\|e\|^2 + \gamma^2\|\nabla e\|^2 &\le \theta_c\|\psi''(u_1)\|_{L^\infty(\Omega)}\|e\|^2 + \theta_c\|g(u_1)\|_{L^\infty(\Omega)}\|e\|_{L^3(\Omega)}^3 \\ &\quad + (1-\gamma^2)\lambda_{AC}\|e\|^2 + (1-\gamma^2)\gamma^{-2}\big(\theta_c\|g(u_1)\|_{L^\infty(\Omega)} + \theta\|\phi'''(u_1)\|_{L^\infty(\Omega)}\big)\|e\|_{L^3(\Omega)}^3 + \langle r,e\rangle.\end{aligned}$$

Estimating

$$2\langle r,e\rangle \le \mu_0^2 + \|e\|^2 + \gamma^{-2}\mu_1^2 + \gamma^2\|\nabla e\|^2$$

and integrating over $(0,t)$ we have, using $\gamma\le 1$,

$$\begin{aligned}\|e(t)\|^2 + \gamma^2\int_0^t \|\nabla e\|^2\,\mathrm{d}s &\le 2\int_0^t \big(\theta_c\|\psi''(u_1)\|_{L^\infty(\Omega)} + (1-\gamma^2)\lambda_{AC} + 1/2\big)\|e\|^2\,\mathrm{d}s \\ &\quad + 2\gamma^{-2}\int_0^t \big(2\theta_c\|g(u_1)\|_{L^\infty(\Omega)} + \theta\|\phi'''(u_1)\|_{L^\infty(\Omega)}\big)\|e\|_{L^3(\Omega)}^3\,\mathrm{d}s + \int_0^t (\mu_0^2+\gamma^{-2}\mu_1^2)\,\mathrm{d}s + \|e(0)\|^2.\end{aligned}$$

Employing Hölder's inequality to bound $\|e\|_{L^3(\Omega)} \le \|e\|\|e\|^2_{L^4(\Omega)}$ and the Sobolev estimate $\|e\|^2_{L^4(\Omega)} \le C_S^2(\|e\|^2 + \|\nabla e\|^2)$ we find that

$$\int_0^t \|e\|^3_{L^3(\Omega)}\,\mathrm{d}s \le C_S^2 \sup_{s\in(0,t)} \|e\| \int_0^t (\|e\|^2 + \|\nabla e\|^2)\,\mathrm{d}s.$$

We are thus in the situation of Lemma 2.3 with $y_1(t) = \|e(t)\|^2$, $y_2(t) = \gamma^2\|\nabla e(t)\|^2$, $y_3(t) = \gamma^2 C_S^{-2} B\|e(t)\|^3_{L^3(\Omega)}$, $\beta = 1/2$, $A = \int_0^T (\mu_0^2 + \gamma^{-2}\mu_1^2)\,\mathrm{d}s + \|e(0)\|^2$, and α and B as above. This implies the proposition. □

Remark 3.3. *For F as in (2) the function ϕ''' is unbounded at ± 1 while the function ψ'' and g are bounded on $[-1,1]$. Although for positive times t it is known that solutions and appropriate finite element approximations satisfy $\|u(t)\|_{L^\infty(\Omega)} < 1$, the quantity B of the previous proposition may be undefined if the given initial data $u_1(0)$ attains the values ± 1 in a set of nonzero measure. To avoid this, one may apply Lemma 2.3 to (3) in the temporal interval $[0,\gamma^2]$ and then apply the arguments of the proof of Proposition 3.2 in the interval $[\gamma^2, T]$.*

4. Abstract error analysis for Cahn–Hilliard equations

Slightly different arguments are required for an abstract error analysis for the H^{-1} gradient flow of $\mathcal{E}_\gamma$. Throughout this section we set

$$\mathbb{V} := H^1(\Omega), \quad \mathring{\mathbb{V}} := \{\eta \in \mathbb{V} : \overline{\eta} = \frac{1}{|\Omega|}\int_\Omega \eta\,\mathrm{d}x = 0\}$$

and

$$X_{CH} := (H^1(0,T;\mathbb{V}') \cap L^2(0,T;\mathbb{V})) \times L^2(0,T;\mathbb{V}).$$

Given $v \in L^2(\Omega)$ with $\overline{v} = 0$ we let $-\Delta_N^{-1} v$ denote the unique function in $\mathring{\mathbb{V}}$ that satisfies

$$(\nabla(-\Delta_N^{-1} v), \nabla\chi) = (v, \chi)$$

for all $\chi \in \mathbb{V}$.

Lemma 4.1. *There exists $C_I > 0$ such that for all $\eta \in \mathring{\mathbb{V}}$ if $d = 2$ and for all $\eta \in \mathring{\mathbb{V}} \cap L^\infty(\Omega)$ if $d = 3$ we have*

$$\|\eta\|^3_{L^3(\Omega)} \le C_I \|\eta\|^{1-\sigma}_{L^\infty(\Omega)} \|\nabla\Delta_N^{-1}\eta\|^\sigma \|\nabla\eta\|^2$$

where $\sigma = 1$ if $d = 2$ and $\sigma = 4/5$ if $d = 3$.

Proof. Suppose first that $d = 2$ and $\sigma = 1$. Then, Hölder's inequality and the multiplicative Sobolev inequality $\|\eta\|^2_{L^4(\Omega)} \le C\|\eta\|\|\nabla\eta\|$, cf. [LU68, (2.10)], yield that

$$\|\eta\|^3_{L^3(\Omega)} \le \|\eta\|\|\eta\|^2_{L^4(\Omega)} \le C\|\eta\|^2\|\nabla\eta\|.$$

Owing to the definition of $-\Delta_N^{-1}$ we have that

$$\|\eta\|^2 = (\nabla(-\Delta_N^{-1}\eta), \nabla\eta) \le \|\nabla\Delta_N^{-1}\eta\|\|\nabla\eta\| \tag{6}$$

and this implies the asserted result. If $d = 3$ and $\sigma = 4/5$ we have

$$\|\eta\|^3_{L^3(\Omega)} \le \|\eta\|^{1-\sigma}_{L^\infty(\Omega)} \int_\Omega |\eta|^{2+\sigma}\,\mathrm{d}x$$

and, upon applying Hölder's inequality with exponents $1/\sigma$ and $1/(1-\sigma)$,

$$\int_\Omega |\eta|^{2+\sigma}\,\mathrm{d}x \le \||\eta|^{2\sigma}\|_{L^{1/\sigma}(\Omega)} \||\eta|^{2-\sigma}\|_{L^{1/(1-\sigma)}(\Omega)} = \|\eta\|^{2\sigma}\|\eta\|^{2-\sigma}_{L^{(2-\sigma)/(1-\sigma)}(\Omega)}.$$

The Sobolev inequality $\|\eta\|_{L^6(\Omega)} \le C_S\|\nabla\eta\|$ implies

$$\|\eta\|_{L^3(\Omega)} \le \|\eta\|_{L^\infty(\Omega)}^{1-\sigma}\|\eta\|^{2\sigma}C_S^{2-\sigma}\|\nabla\eta\|^{2-\sigma}$$

and the combination with (6) leads to the asserted result for $d=3$. □

Definition 4.2. *a) For $\ell=1,2$ let $(u_\ell,w_\ell)\in X_{CH}$ and set $\widetilde{u}_\ell := u_\ell - \overline{u}_\ell + \overline{u}_0$ for given $\overline{u}_0\in\mathbb{R}$. Assume that $\|u_\ell(t)\|_{L^\infty(\Omega)}\le C_\infty$ for $\ell=1,2$ and almost every $t\in[0,T]$ if $d=3$ and define the* residuals *$r_\ell,s_\ell\in L^2(0,T;\mathbb{V}')$ such that*

$$\begin{aligned}\langle r_\ell,\eta\rangle &= \langle\partial_t\widetilde{u}_\ell,\eta\rangle + (\nabla w_\ell,\nabla\eta),\\ \langle s_\ell,\chi\rangle &= -(w_\ell,\chi)+\gamma(\nabla\widetilde{u}_\ell,\nabla\chi)+\gamma^{-1}(f(\widetilde{u}_\ell),\chi)\end{aligned}$$

for all $(\eta,\chi)\in\mathbb{V}^2$ and almost everywhere in $[0,T]$. If $r_\ell,s_\ell=0$ almost everywhere in $[0,T]$, we call u_ℓ a weak solution of the Cahn–Hilliard equation.
b) For almost every $t\in[0,T]$ let the principal eigenvalue *$-\lambda_{CH}(t)$ be defined through*

$$-\lambda_{CH}(t) := \inf_{\eta\in\overset{\circ}{\mathbb{V}}\setminus\{0\}} \frac{\gamma\|\nabla\eta\|^2+\gamma^{-1}\big(f'(\widetilde{u}_1(t))\eta,\eta\big)}{\|\nabla\Delta_N^{-1}\eta\|^2}. \tag{7}$$

c) Set $e:=\widetilde{u}_1-\widetilde{u}_2$, $z:=-\Delta_N^{-1}e$, $\delta:=w_1-w_2$ and $r:=r_1-r_2$, $s:=s_1-s_2$ and assume that there exist functions $\mu_{-1},\mu_0,\mu_1:[0,T]\to\mathbb{R}$ called residual estimators *such that*

$$\langle r(t),\eta\rangle+\langle s(t),\chi\rangle \le \mu_{-1}(t)\|\nabla\eta\|+\mu_0(t)\|\chi\|+\mu_1(t)\|\nabla\chi\|.$$

for almost every $t\in[0,T]$ and all $(\eta,\chi)\in\overset{\circ}{\mathbb{V}}\times\mathbb{V}$.

Remark 4.3. *Although a maximum principle is false in general for Cahn–Hilliard equations it is possible to prove uniform a priori bounds in $L^\infty(0,T;L^\infty(\Omega))$, cf.* [CM95]. *Hence, the assumption $\|\widetilde{u}_\ell(t)\|_{L^\infty(\Omega)}\le C$ if $d=3$ is not restrictive. For logarithmic potentials, this bound is trivially satisfied. The assumption can be avoided if certain growth conditions are imposed on f, cf.* [BM10a].

Proposition 4.4. *Let (GA) hold, assume $0<\gamma\le 1$, and there are residual estimators μ_{-1}, μ_0,μ_1 according to Definition 4.2. For almost every $t\in[0,T]$ define*

$$\begin{aligned}\alpha(t) &:= 2\big(2\theta_c^2\|\psi''(\widetilde{u}_1)\|_{L^\infty(\Omega)}^2+(1-\gamma^3)\lambda_{CH}+1\big)^+,\\ B &:= 4\gamma^{-5}\big(C_I 4^{1-\sigma}C_\infty^{1-\sigma}\big)\sup_{s\in[0,T]}\big(2\theta_c\|g(\widetilde{u}_1(s))\|_{L^\infty(\Omega)}+\theta\|\phi'''(\widetilde{u}_1(s))\|_{L^\infty(\Omega)}\big)\end{aligned}$$

and suppose that with $E:=\exp\big(\int_0^T\alpha(s)\,\mathrm{d}s\big)$ we have

$$\int_0^T\big(\mu_{-1}^2+\gamma^{-2}\mu_0^2+\gamma^{-4}\mu_1^2\big)\,\mathrm{d}s+\|\nabla z(0)\|^2 \le (8E)^{-(1+2/\sigma)}B^{-2/\sigma}(1+T)^{-2/\sigma},$$

where $\sigma=1$ if $d=2$ and $\sigma=4/5$ if $d=3$. Then we have

$$\begin{aligned}\sup_{s\in[0,T]}\|\nabla z(s)\|^2+\frac{\gamma^4}{2}\int_0^T\|\nabla e\|^2\,\mathrm{d}s \le 8\Big(\int_0^T\big(\mu_{-1}^2+\gamma^{-2}\mu_0^2+\gamma^{-4}\mu_1^2\big)\,\mathrm{d}s+\|\nabla z(0)\|^2\Big)\\ \times\exp\Big(2\int_0^T\big(2\theta_c\|\psi''(\widetilde{u}_1)\|_{L^\infty(\Omega)}^2+(1-\gamma^3)\lambda_{CH}+1\big)^+\,\mathrm{d}s\Big).\end{aligned}$$

Proof. We subtract the equations for $(\widetilde{u}_1,w_1)$ and $(\widetilde{u}_2,w_2)$ and choose $\eta=z$ and $\chi=e$ to verify

$$\begin{aligned}\langle\partial_t e,z\rangle+(\nabla\delta,\nabla z) &= \langle r,z\rangle,\\ -(\delta,e)+\gamma(\nabla e,\nabla e) &= -\gamma(f(\widetilde{u}_1)-f(\widetilde{u}_2),e)+\langle s,e\rangle.\end{aligned}$$

Using that $2\langle\partial_t e,z\rangle=\frac{d}{dt}\|\nabla z\|^2$ and $(\nabla\delta,\nabla z)=(\delta,e)$, we find upon adding the two equations that

$$\frac12\frac{d}{dt}\|\nabla z\|^2+\gamma\|\nabla e\|^2=-\gamma^{-1}(f(\widetilde{u}_1)-f(\widetilde{u}_2),e)+\langle r,z\rangle+\langle s,e\rangle.$$

The assumed estimate for ψ and the monotonicity of ϕ' lead to, cf. (3),

$$\frac12\frac{d}{dt}\|\nabla z\|^2+\gamma\|\nabla e\|^2\le\gamma^{-1}\theta_c\|\psi''(\widetilde{u}_1)\|_{L^\infty(\Omega)}\|e\|^2+\gamma^{-1}\theta_c\|g(\widetilde{u}_1)\|_{L^\infty(\Omega)}\|e\|^3_{L^3(\Omega)}+\langle r,z\rangle+\langle s,e\rangle. \tag{8}$$

Alternatively, using that

$$(f(a)-f(b))(a-b)\ge f'(a)(a-b)^2-\theta_c g(a)(a-b)^3-\theta\phi'''(a)(a-b)^3/2$$

for all $a,b\in I$, cf. (4), and incorporating the definition of λ_{CH}, we find that

$$\begin{aligned}&\frac12\frac{d}{dt}\|\nabla z\|^2+\gamma\|\nabla e\|^2\\ &\le-\gamma^{-1}(f'(\widetilde{u}_1)e,e)+\gamma^{-1}\big(\theta_c\|g(\widetilde{u}_1)\|_{L^\infty(\Omega)}+\theta\|\phi'''(\widetilde{u}_1)\|_{L^\infty(\Omega)}\big)\|e\|^3_{L^3(\Omega)}+\langle r,z\rangle+\langle s,e\rangle\\ &\le\lambda_{CH}\|\nabla z\|^2+\gamma\|\nabla e\|^2+\gamma^{-1}\big(\theta_c\|g(\widetilde{u}_1)\|_{L^\infty(\Omega)}+\theta\|\phi'''(\widetilde{u}_1)\|_{L^\infty(\Omega)}\big)\|e\|^3_{L^3(\Omega)}+\langle r,z\rangle+\langle s,e\rangle.\end{aligned} \tag{9}$$

We multiply (8) by γ^3 and (9) by $(1-\gamma^3)$ and add the resulting estimates to deduce that

$$\begin{aligned}\frac12\frac{d}{dt}\|\nabla z\|^2+\gamma^4\|\nabla e\|^2&\le\gamma^2\theta_c\|\psi''(\widetilde{u}_1)\|_{L^\infty(\Omega)}\|e\|^2+\gamma^2\theta_c\|g(\widetilde{u}_1)\|_{L^\infty(\Omega)}\|e\|^3_{L^3(\Omega)}+(1-\gamma^3)\lambda_{CH}\|\nabla z\|^2\\ &\quad+(1-\gamma^3)\gamma^{-1}\big(\theta_c\|g(\widetilde{u}_1)\|_{L^\infty(\Omega)}+\theta\|\phi'''(\widetilde{u}_1)\|_{L^\infty(\Omega)}\big)\|e\|^3_{L^3(\Omega)}+\langle r,z\rangle+\langle s,e\rangle.\end{aligned}$$

We employ $\gamma\le1$, bound

$$2\langle r,z\rangle+2\langle s,e\rangle\le\mu_{-1}^2+\|\nabla z\|^2+\gamma^{-2}\mu_0^2+\gamma^2\|e\|^2+\gamma^{-4}\mu_1^2+\gamma^4\|\nabla e\|^2,$$

use that $\|e\|^2\le\|\nabla z\|\|\nabla e\|$ to estimate

$$\gamma^2\|e\|^2+2\gamma^2\theta_c\|\psi''(\widetilde{u}_1)\|_{L^\infty(\Omega)}\|e\|^2\le\frac{\gamma^4}{4}\|\nabla e\|^2+\|\nabla z\|^2+\frac{\gamma^4}{4}\|\nabla e\|^2+4\theta_c^2\|\psi''(\widetilde{u}_1)\|^2_{L^\infty(\Omega)}\|\nabla z\|^2,$$

and integrate over $(0,t)$ to verify that

$$\begin{aligned}&\|\nabla z(t)\|^2+\frac{\gamma^4}{2}\int_0^t\|\nabla e\|^2\,\mathrm{d}s\le2\int_0^t\big(2\theta_c^2\|\psi''(\widetilde{u}_1)\|^2_{L^\infty(\Omega)}+(1-\gamma^3)\lambda_{CH}+1\big)\|\nabla z\|^2\,\mathrm{d}s\\ &+2\gamma^{-1}\int_0^t\big(2\theta_c\|g(\widetilde{u}_1)\|_{L^\infty(\Omega)}+\theta\|\phi'''(\widetilde{u}_1)\|_{L^\infty(\Omega)}\big)\|e\|^3_{L^3(\Omega)}\,\mathrm{d}s+\int_0^t\big(\mu_{-1}^2+\gamma^{-2}\mu_0^2+\gamma^{-4}\mu_1^2\big)\,\mathrm{d}s+\|\nabla z(0)\|^2.\end{aligned}$$

We use Lemma 4.1 and the bound $\|e\|_{L^\infty(\Omega)}\le4C_\infty$ if $d=3$ to control

$$\int_0^t\|e\|^3_{L^3(\Omega)}\,\mathrm{d}s\le C_I4^{1-\sigma}C_\infty^{1-\sigma}\sup_{s\in(0,t)}\|\nabla z\|^\sigma\int_0^t\|\nabla e\|^2\,\mathrm{d}s.$$

We are thus in the situation of Lemma 2.3 with $y_1(t)=\|\nabla z(t)\|^2$, $y_2(t)=(\gamma^4/2)\|\nabla e(t)\|^2$, $y_3(t)=(\gamma^4/2)(C_I4^{1-\sigma}C_\infty^{1-\sigma})^{-1}B\|e(t)\|^3_{L^3(\Omega)}$, $\beta=\sigma/2$, $A=\int_0^T\big(\mu_{-1}^2+\gamma^{-2}\mu_0^2+\gamma^{-4}\mu_1^2\big)\,\mathrm{d}s+\|\nabla z(0)\|^2$, and α and B as above. This implies the proposition. □

5. Quasi-optimal error estimates for non-standard finite element methods

For conforming finite element methods, the derivation of error estimates in the energy norm follows from the abstract theory with standard arguments and we refer the reader to [KNS04, Bar05, BM10a, BM10b] for related estimates. We discuss in this section error estimates in $L^\infty(0,T;L^2(\Omega))$ for the Allen–Cahn problem and in $L^\infty(0,T;\mathbb{V}')$ for Cahn–Hilliard evolutions allowing a large class of non-standard finite element methods such as discontinuous Galerkin, mixed, or non-conforming methods. These estimates do not follow directly from the abstract theory. The key to such estimates

is an appropriate conforming reconstruction of the approximate solution to which the abstract theory of the previous sections can be applied. The resulting estimates are of particular importance for phase field models since they lead to weaker conditions under which the abstract error estimates of the previous sections hold. Moreover, it demonstrates how techniques that were developed for linear second order problems can be carried over to nonlinear and fourth order problems.

For ease of presentation we restrict ourselves to implicit discretizations in time and omit the question of the approximate solution of the resulting nonlinear systems of equations. Throughout the following suppose that we are given time steps

$$0 = t_0 < t_1 < ... < t_J = T$$

and for $j = 0, 1, ..., J$ a discretization of the Laplace operator given by a bilinear form $a_h^j : \mathbb{V}_h^j \times \mathbb{V}_h^j \to \mathbb{R}$ which defines the discrete Laplace operator $-\Delta_h^j : \mathbb{V}_h^j \to L^2(\Omega)$ on the possibly non-conforming finite element space $\mathbb{V}_h^j$ via

$$(-\Delta_h^j V, W) = a_h^j(V, W)$$

for all $W \in \mathbb{V}_h^j$. We let $P_h^j : L^2(\Omega) \to \mathbb{V}_h^j$ be the L^2 projection onto $\mathbb{V}_h^j$ and denote by d_t the backward difference operator defined for any sequence $(a^j)_{j=0,...,J}$ by $d_t a^j = (a^j - a^{j-1})/(t_j - t_{j-1})$, $j = 1, 2, ..., J$.

5.1. **Estimates in $L^\infty(0,T;L^2(\Omega))$ for the Allen–Cahn problem.** Assume we are given approximate solutions $(U^j)_{j=0,...,J} \subset L^2(\Omega)$ which satisfy for $j = 1, 2, ..., J$ that $U^j \in \mathbb{V}_h^j$ and

$$d_t U^j - \Delta_h^j U^j = -\gamma^{-2} P_h^j f(U^j), \tag{10}$$

For $j = 0, 1, ..., J$ we let $\widehat{u}^j \in H^1(\Omega)$ be the weak solution of

$$-\Delta \widehat{u}^j = -\Delta_h^j U^j \text{ in } \Omega, \qquad \nabla \widehat{u}^j \cdot \nu = 0 \text{ on } \partial\Omega, \qquad \int_\Omega \widehat{u}^j \,\mathrm{d}x = \int_\Omega U^j \,\mathrm{d}x.$$

The function $\widehat{u} : (0,T) \to \mathbb{V}$ is obtained by piecewise linear interpolation in time of the functions $(\widehat{u}^j)_{j=0,...,J}$. The abstract theory of Section 3 can be applied to the function $\widehat{u}$ provided that we can control the residual

$$\langle r, \eta \rangle = \langle \partial_t \widehat{u}, \eta \rangle + (\nabla \widehat{u}, \nabla \eta) + \gamma^{-2}(f(\widehat{u}), \eta).$$

Owing to (10) and the definition of $\widehat{u}^j$ we have for $t_{j-1} < t < t_j$ that

$$\begin{aligned}\langle r, \eta \rangle = (\partial_t(\widehat{u} - U), \eta) + (\nabla[\widehat{u} - \widehat{u}^j], \nabla \eta) + \gamma^{-2}(f(\widehat{u}) - f(\widehat{u}^j), \eta) \\ + \gamma^{-2}(f(\widehat{u}^j) - f(U^j), \eta) + \gamma^{-2}(f(U^j) - P_h f(U^j), \eta).\end{aligned}$$

Controlling this residual requires to bound the difference $\widehat{u} - U$ in different norms. This however is fairly standard since U^j is the finite element approximation of the Poisson problem whose exact solution is $\widehat{u}^j$ but requires to guarantee H^2 regularity of the Laplace operator in Ω subject to homogeneous Neumann boundary conditions. Moreover, a weak mesh-compatibility condition has to be assumed in order to bound the quantity $\|d_t \widehat{u}^j - d_t U^j\|$. We refer the reader to [BM10b] for related details. These arguments lead to error control for the difference $\widehat{u} - u$ and an application of the triangle inequality implies an error estimate for $\widehat{u} - u$, where U is the linear interpolation in time of the iterates $(U^j)_{j=0,...,J}$. The resulting estimates are quasi-optimal for the error in the norm $L^\infty(0,T;L^2(\Omega))$.

We remark that if the approximate solution U is employed directly to define the residual then we have for $t_{j-1} < t < t_j$ and all $\eta \in \mathbb{V}$ and $\eta_h \in \mathbb{V}_h^j$ that

$$\begin{aligned}\langle r, \eta\rangle &= (\partial_t U, \eta) + (\nabla U, \nabla\eta) + \gamma^{-2}(f(U), \eta)\\ &= (d_t U^j, \eta) + (\nabla U^j, \nabla\eta) + \gamma^{-2}(f(U^j), \eta) + (\nabla[U - U^j], \nabla\eta) + \gamma^{-2}(f(U) - f(U^j), \eta)\\ &= (d_t U^j, \eta - \eta_h) + (\nabla U^j, \nabla(\eta - \eta_h)) + \gamma^{-2}(f(U^j), \eta - \eta_h)\\ &\quad + (\nabla[U - U^j], \nabla\eta) + \gamma^{-2}(f(U) - f(U^j), \eta)\end{aligned}$$

provided that $\mathbb{V}_h^j \subset \mathbb{V}$ for $j = 1, 2, ..., J$. Letting η_h be a weak interpolant of η we obtain an estimate for the residual in a standard way, cf., e.g., [BMO09]. The second term on the right-hand side leads to an upper bound which is only of first order with respect to the spatial discretization and hence suboptimal for an error analysis in $L^\infty(0, T; L^2(\Omega))$.

5.2. **Estimates in $L^\infty(0, T; \mathbb{V}')$ for the Cahn–Hilliard problem.** Assume we are given approximate solutions $(U^j, W^j)_{j=0,...,J} \subset L^2(\Omega)^2$ which satisfy for $j = 1, 2, ..., J$

$$d_t U^j - \Delta_h^j W^j = 0, \qquad W^j = -\gamma \Delta_h^j U^j + \gamma^{-1} P_h^j f(U^j). \tag{11}$$

For $j = 0, 1, ..., J$ we let $\widehat{u}^j, \widehat{w}^j \in H^1(\Omega)$ be the weak solutions of

$$\begin{aligned}&-\Delta\widehat{u}^j = -\Delta_h U^j \text{ in } \Omega, \qquad \nabla\widehat{u}^j \cdot \nu = 0 \text{ on } \partial\Omega, \qquad \int_\Omega \widehat{u}^j \,\mathrm{d}x = \int_\Omega U^j \,\mathrm{d}x,\\ &-\Delta\widehat{w}^j = -\Delta_h W^j \text{ in } \Omega, \qquad \nabla\widehat{w}^j \cdot \nu = 0 \text{ on } \partial\Omega, \qquad \int_\Omega \widehat{w}^j \,\mathrm{d}x = \int_\Omega W^j \,\mathrm{d}x.\end{aligned}$$

We may then apply the abstract theory of Section 4 to the piecewise linear interpolations $\widehat{u}$ and $\widehat{w}$ of $(\widehat{u}^j)_{j=0,...,J}$ and $(\widehat{w}^j)_{j=0,...,J}$. For a practical error control we need to estimate the residuals defined by the reconstructions $\widehat{u}$ and $\widehat{w}$.

$$\begin{aligned}\langle r, \eta\rangle &= \langle \partial_t \widehat{u}, \eta\rangle + (\nabla\widehat{w}, \nabla\eta),\\ \langle s, \chi\rangle &= -(\widehat{w}, \chi) + \gamma(\nabla\widehat{u}, \nabla\chi) + \gamma^{-1}(f(\widehat{u}), \chi).\end{aligned}$$

Owing to (11) and the choice of $\widehat{u}^j$ and $\widehat{w}^j$ we have for $t_{j-1} < t < t_j$ that

$$\langle r, \eta\rangle = (\partial_t \widehat{u} - d_t U^j, \eta) + (\nabla[\widehat{w} - \widehat{w}^j], \nabla\eta)$$

and

$$\begin{aligned}(s, \chi) = -(\widehat{w} - \widehat{w}^j, \chi) + \gamma(\nabla[\widehat{u} - \widehat{u}^j], \nabla\chi) + \gamma^{-1}(f(\widehat{u}) - f(\widehat{u}^j), \chi)\\ + \gamma^{-1}(f(\widehat{u}^j) - f(U^j), \chi) + \gamma^{-1}(f(U^j) - P_h f(U^j), \chi).\end{aligned}$$

The second term on the right-hand side in the identity for r and the first three terms on the right-hand side in the identity for s are time-discretization residuals, while the remaining terms correspond to errors induced by discretization in space. Again, we refer the reader to [BM10b] for details. The abstract theory of Section 4.4 and an application of the triangle inequality then lead to error estimates between the approximate solution (U, W) and the exact solution (u, w) which are quasi-optimal in the norm of $L^\infty(0, T; \mathbb{V}')$.

6. Numerical experiments

The goals of this section are (i) to numerically verify the logarithmic bounds for the time integrated principal eigenvalue Λ_{CH} past topological changes and (ii) to analyze the dependence of the solution on the temperature θ. The qualitative behavior of $\Lambda_{CH}(t)$ for smooth potentials was previously studied in [BM10a], where in the event of topological changes peaks of height proportional to γ^{-1} were observed. The temporal discretization parameters employed there were not sufficiently fine to draw conclusions about the time integrated eigenvalue. For the Allen–Cahn equation with quartic potential, robust error control past topological changes was established in [BMO09]. The corresponding results for logarithmic potentials are presented here in Section 6.2.4.

In the experiments below, we use lowest order continuous finite elements on a uniform triangular grid and a constant time step size τ. For adaptive strategies we refer to [Bar05, BM10a, BM10b] but remark that the residual estimators in the Propositions 3.2 and 4.4 provide local indicators for grid adaption in a natural way. To further simplify the numerical scheme we apply mass lumping defined for continuous functions $v, w \in C(\overline{\Omega})$ and the nodal interpolation operator $\mathcal{I}_h$ related to the finite element space $\mathbb{V}_h$ by $(v,w)_h = \int_\Omega \mathcal{I}_h[vw]\,\mathrm{d}x$. The implicit Euler method in time then leads to the following discrete problem:

$$(\mathrm{CH_h}) \qquad \begin{cases} \text{Given } U^0 \in \mathbb{V}_h, \text{ for } j = 1,2,\ldots \text{ find } (U^j, W^j) \in \mathbb{V}_h \times \mathbb{V}_h \text{ such that} \\ \quad (U^j,\eta) + \tau\,(\nabla W^j, \nabla\eta) = (\eta, U^{j-1}\eta)\,, \\ \quad -\gamma\,(\nabla U^j, \nabla\chi) - \gamma^{-1}\,(f(U^j),\chi)_h + (W^j,\chi) = 0 \\ \text{for all } \eta \in \mathbb{V}_h \text{ and all } \chi \in \mathbb{V}_h. \end{cases}$$

Within each time step the nonlinear system is solved by Newton's method. The eigenvalue Λ_{CH} is approximated by the principal eigenvalue of the operator related to $(\mathrm{CH_h})$. The discrete eigenvalue problem reads

$$(\mathrm{EV_h}) \qquad \begin{cases} \text{Find } (V, Z, \Lambda_{CH}) \in \mathbb{V}_h \times \mathbb{V}_h \times \mathbb{R} \text{ such that} \\ \quad (V,\eta) - (\nabla Z, \nabla\eta) = 0\,, \\ \quad \gamma\,(\nabla V, \nabla\chi) + \gamma^{-1}\,(f'(U^j)V,\chi)_h + \alpha\,(Z,\chi)_h = (\alpha_\gamma - \Lambda_{CH})\,(Z,\chi)_h \\ \text{for all } \eta \in \mathbb{V}_h \text{ and all } \chi \in \mathbb{V}_h. \end{cases}$$

Here, the constant $\alpha_\gamma \in \mathbb{R}$ is a shift to guarantee that the left hand side in $(\mathrm{EV_h})$ defines a positive definite matrix such that $(\mathrm{EV_h})$ can be solved by an inverse vector iteration. The necessary shift is determined by an a priori upper bound for Λ_{CH}. By (GA) and the additional assumption $-f'(u) \le C_f$ for some $C_f > 0$, we have

$$\begin{aligned} -\gamma\|\nabla\eta\|^2_{L^2(\Omega)} - \gamma^{-1}(\eta, f'(\tilde{u}_1)\eta) &\le -\gamma\|\nabla\eta\|^2_{L^2(\Omega)} + \gamma^{-1} C_f \|\eta\|^2_{L^2(\Omega)} \\ &\le -\gamma\|\nabla\eta\|^2_{L^2(\Omega)} + \gamma^{-1} C_f \|\nabla\eta\|_{L^2(\Omega)} \|\nabla\Delta_N^{-1}\eta\|_{L^2(\Omega)} \\ &\le \frac{\gamma^{-3} C_f^2}{4} \|\nabla\Delta_N^{-1}\eta\|^2_{L^2(\Omega)}\,, \end{aligned}$$

where in the last step, we applied Young's inequality with the constant $2\gamma^2/C_f$. We conclude

$$\lambda_{CH} = \sup_{\eta \in \mathbb{V}\setminus\{0\}} \frac{-\gamma\|\nabla\eta\|^2_{L^2(\Omega)} - \gamma^{-1}(f'(\tilde{u}_1)\eta,\eta)}{\|\nabla\Delta_N^{-1}\eta\|^2_{L^2(\Omega)}} \le \frac{\gamma^{-3} C_f^2}{4} =: \alpha_\gamma\,. \tag{12}$$

For the potential (2) we have $C_f = \theta_c - \theta$ and in the smooth quartic case $C_f = 1$.

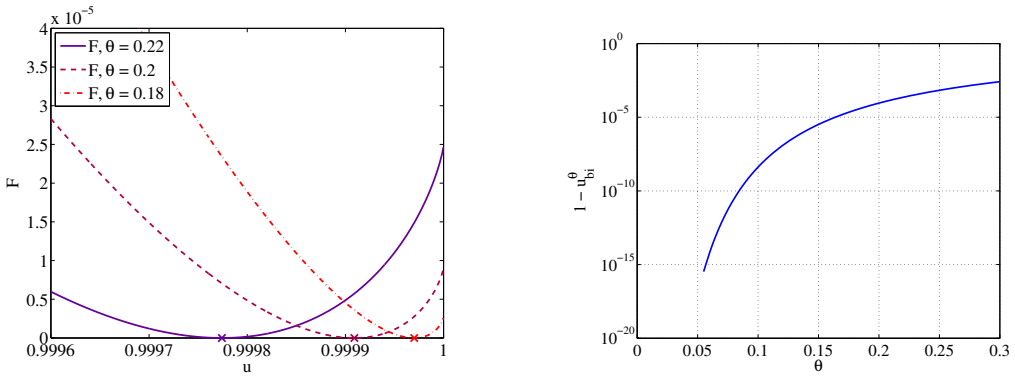

FIGURE 2. Zoom of the logarithmic potential F around the binodal point $u_{\rm bi}^\theta$ (indicated by crosses) for $\theta_c = 1$ and different θ (left). For $\theta \to 0$, the distance $1 - u_{\rm bi}^\theta$ reduces rapidly and reaches IEEE floating point accuracy already for $\theta \approx 0.05\,\theta_c$ (right).

6.1. **Iterative solution via regularization.** The potential F from (2) has a double well structure where the location of the minima defines the *binodal points* $\pm u_{\rm bi}^\theta$, see Figures 1 and 2. These points determine the values of the solution within the bulk phases whereas the singularities of F at ± 1 guarantee that $|u| < 1$. For $\theta \to 0$, the binodal points $u_{\rm bi}^\theta$ converge rapidly to the singular points at ± 1. Figure 2 shows that already for moderate temperatures like $\theta = 0.05\,\theta_c$ we have $1 - u_{\rm bi}^\theta \approx 10^{-16}$. Then, the binodal points can not be distinguished from the singularities of F within the range of IEEE floating point accuracy what makes a meaningful simulation impossible.

The practical solution of the discrete system $(\mathrm{CH_h})$ requires a regularization of the potential at the singular points. For $\varepsilon > 0$, we follow [BB95] and define $F_\varepsilon(u) = \theta\phi_\varepsilon(u) - \theta_c u^2/2$ with

$$2\phi_\varepsilon(u) = \begin{cases} (1+u)\ln(1+u) + (1-u)\ln(1-u) & \text{if } |u| < 1-\varepsilon, \\ (1+u)\ln(1+u) + (1-u)^2/(2\varepsilon) + (1-u)\ln(\varepsilon) - \varepsilon/2 & \text{if } u \geq 1-\varepsilon, \\ (1-u)\ln(1-u) + (1+u)^2/(2\varepsilon) + (1+u)\ln(\varepsilon) - \varepsilon/2 & \text{if } u \leq -1+\varepsilon. \end{cases} \tag{13}$$

The regularization parameter ε has to be chosen small enough so that it is feasible to define a residual, i.e., that $|u| < 1$ is guaranteed. On the other hand, if ε is small and $|u| > 1-\varepsilon$, then the term $f_\varepsilon'(u) \sim 1/\varepsilon$ in the Newton scheme is of very different order of magnitude compared to the other terms causing numerical difficulties when solving the nonlinear system. If $\varepsilon \leq 1 - |u_{\rm bi}^\theta|$ the minima of the $F_\varepsilon(u)$ coincide with the binodal points. Otherwise, the minima are moved closer to the critical values $u = \pm 1$ or there might even be no minimum at all in the interval $(-1, 1)$. Within each time step of $(\mathrm{CH_h})$ we iteratively decrease the regularization parameters by carrying out the following steps:

(a) If $\varepsilon^j < u_{\rm bi}^\theta/2$ set $\varepsilon^j := 2\,\varepsilon^{j-1}$ else set $\varepsilon^j = \varepsilon^{j-1}$.
(b) Find $(U_{h,\varepsilon^j}^j, W_{h,\varepsilon^j}^j) \in \mathbb{V}_h \times \mathbb{V}_h$ according to $(\mathrm{CH_h})$.
(c) If $\|U_{h,\varepsilon^j}^j\|_{L^\infty(\Omega)} \geq 1 - \varepsilon^j/2$, set $\varepsilon^j := \varepsilon^j/2$ and repeat (c).
(d) Set $j = j+1$ and proceed with (a).

6.2. **Robust error control past topological changes.** During the coarsening by Cahn–Hilliard evolution, several topological changes of the solution occur. In Figure 3 we see the absorption of a small particle by the neighboring larger ones (a), closing of voids (c) and merging of neighboring particles (m,M). For each of these three cases we study a prototypical example of one isolated topological change. We expect that our estimates can be modified by employing a partition of

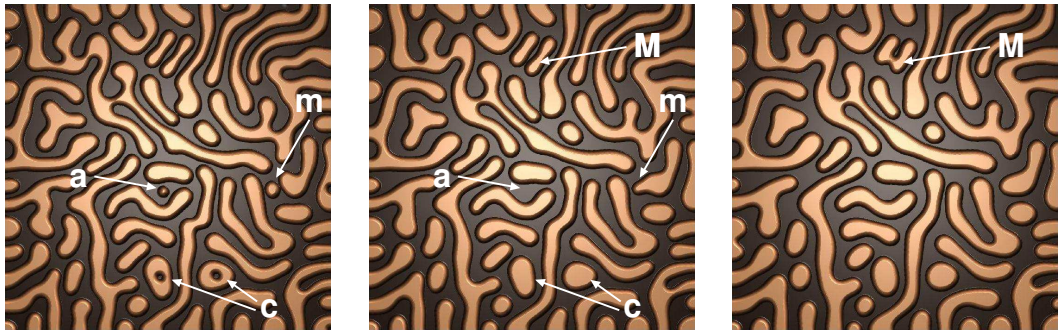

FIGURE 3. Simulation of coarsening by Cahn–Hilliard evolution with $\theta_c = 1$, $\theta = 0.2$ and $\gamma = 1/64$ on the domain $\Omega = (-2,2)^2$. Different topological changes of the solution between the snapshots are marked (a=absorption of a particle, c=closing of voids, m,M=merging of particles).

unity so that localized eigenvalues may be utilized. The goal is to illustrate that in each case the quantity

$$\widetilde{E} := \exp\left(\int_0^T \Lambda_{CH}^+(s)\,\mathrm{d}s\right) \tag{14}$$

and hence the quantity E from Proposition 4.4 depends on γ^{-1} only in a low order polynomial. In the following numerical experiments, the critical temperature is always normalized to $\theta_c = 1$.

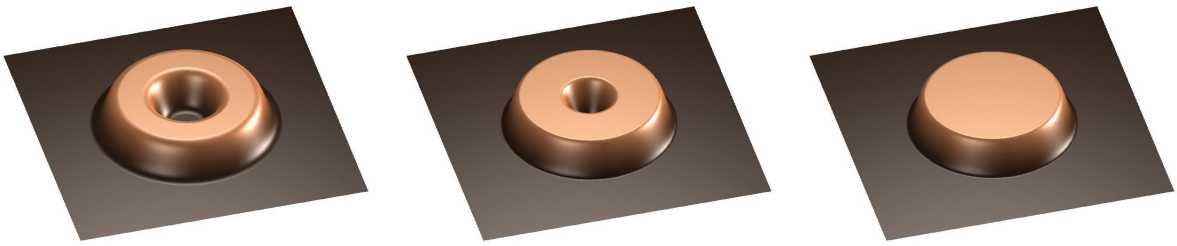

FIGURE 4. Closing of a void: snapshots of the solution from a simulation with $\theta = 0.2$ and $\gamma = 1/32$ at time $t = 0$, $t = 0.005$ and $t = 0.009$.

6.2.1. *Closing of a void.* We prescribe initial values representing interfaces given by concentric circles, see Figure 4. Under Cahn–Hilliard evolution, both interfaces shrink until at some time the inner interface vanishes and the solution reaches a steady state with only one circular interface. Let $\Omega := (-1,1)^2$, $r_1 := 0.2$, $r_2 := 0.55$ and define $d_j(x) := |x| - r_j$ for $x \in \Omega$ and $j = 1,2$. For given $\gamma > 0$ and $x \in \Omega$ let $u_0(x) := \max\left\{-u_{\mathrm{bi}}^\theta, \min\{\tilde{u}_0, u_{\mathrm{bi}}^\theta\}\right\}$ with

$$\tilde{u}_0(x) := -\tanh\left(\frac{d(x)}{\sqrt{2}\gamma}\right), \qquad d(x) := \max\{-d_1(x), d_2(x)\}. \tag{15}$$

In Figure 5, the time evolution of $\Lambda_{CH}(t)$ is plotted for $\theta = 0.2$ and $\gamma = 1/16, 1/24, 1/32, 1/48$. Because the initial data do not match the correct profile across the interfaces, Λ_{CH} is large in the beginning but relaxes rapidly to moderate order. When the inner surface vanishes, uniform bounds for the principal eigenvalue break down due to a peak in $\Lambda_{CH}(t)$ of height comparable to γ^{-3}. On

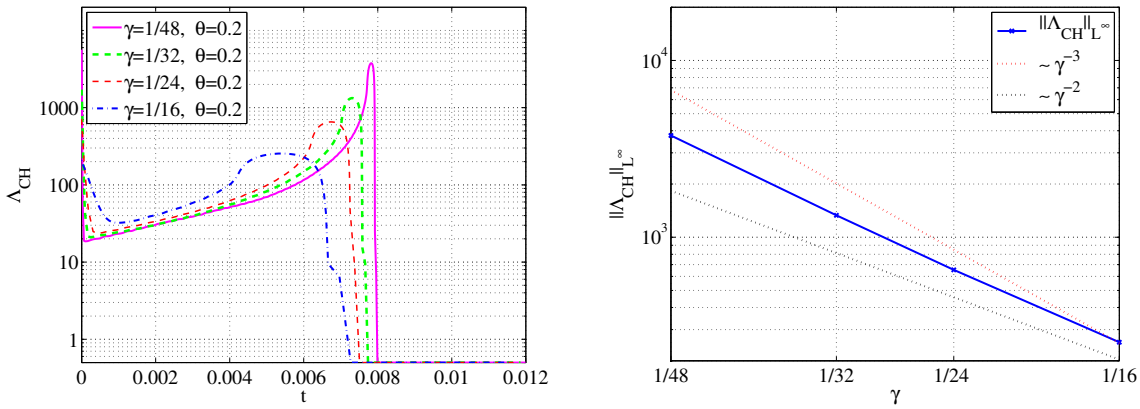

FIGURE 5. Numerically computed eigenvalue $\Lambda_{CH}(t)$ for $\theta = 0.2$ in the closing of a void: a peak of $\Lambda_{CH}(t)$ indicates a topological change in the solution when the inner surface vanishes (left). At the singularities, Λ_{CH} grows comparable to γ^{-3} (right).

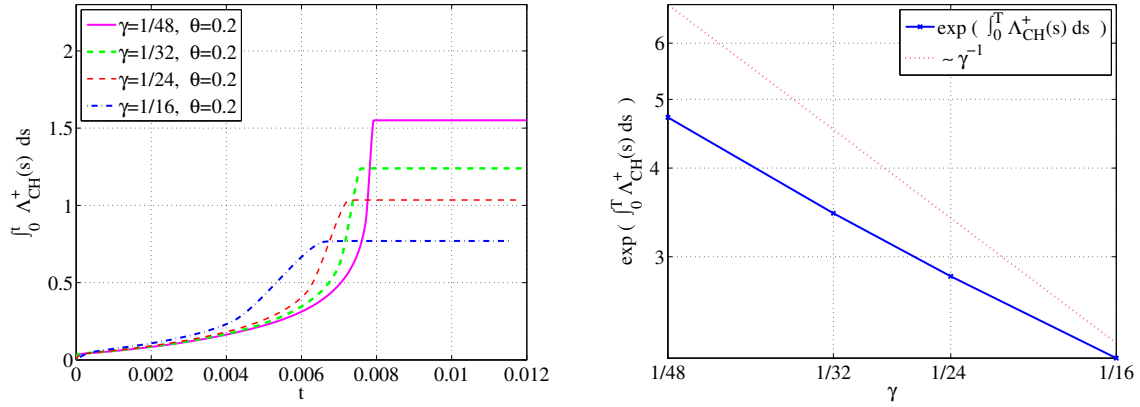

FIGURE 6. Time integrated eigenvalue $L(t) := \int_0^t \Lambda_{CH}^+(s)\,\mathrm{d}s$ for $t \in [0, 0.012]$ in the closing of a void (left). Robust error control past topological changes is possible since growth of $\widetilde{E} = \exp(L(0.012))$ is less than linear in γ^{-1} (right).

the other hand, in Figure 6, the time integrated eigenvalue, i. e. the function L with

$$L(t) := \int_0^t \Lambda_{CH}^+(s)\,\mathrm{d}s \tag{16}$$

shows only a much weaker dependence on γ^{-1}. At $t = 0.012$, we observe that the integrated eigenvalue only grows at a constant rate each time γ is halved. This indicates a logarithmic bound for the time integrated eigenvalue that in turn ensures that for $\gamma \to 0$ the quantity $\widetilde{E}$ according to (14) grows only weaker than some polynomial, in fact less than linear, with respect to γ^{-1}, see Figure 6. Simulations with different values of θ show a similar qualitative behavior, cf. Section 6.3. We conclude that robust error control past topological changes is possible in this prototypical example.

We also compared the results with simulations of the same initial situation, but now using the smooth quartic potential and the initial values $u_0 = \tilde{u}_0$ with $\tilde{u}_0$ as in (15). Figure 7 shows $\Lambda_{CH}(t)$ for $t \in [0, 0.012]$ and $\gamma = 1/16, 1/24, 1/32, 1/48, 1/64$. Again, we observe a peak in $\Lambda_{CH}(t)$ of order γ^{-3} when the inner surface vanishes. Compared to simulations with logarithmic potential, the peak in $\Lambda_{CH}(t)$ occurs later and its position in time converges slower when $\gamma \to 0$. For the time integrated eigenvalue we again observe a logarithmic growth with respect to γ^{-1} leading to a

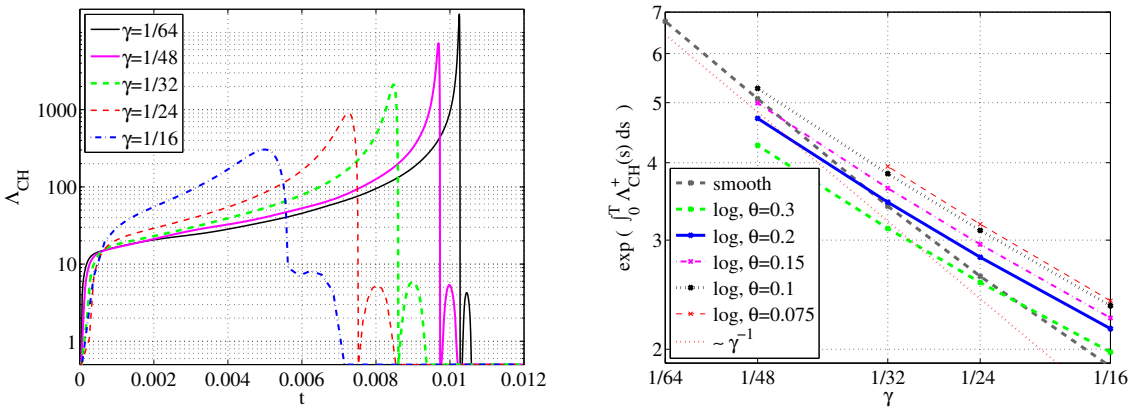

FIGURE 7. Smooth quartic potential: eigenvalue $\Lambda_{CH}(t)$ for $t \in [0, 0.012]$ in the closing of a void (left). Robust error control past topological changes is possible since $\widetilde{E}$ grows only linear with respect to γ^{-1} (right).

linear bound for $\widetilde{E}$, see Figure 7. The solutions of this example approximate for $\gamma \to 0$ a radial symmetric solution of the Mullins–Sekerka problem that can be computed accurately by solving two coupled ordinary differential equations. By comparing to this reference solution, we verified that the finite element solution matches the correct temporal and spatial scales. We convinced ourself that numerical results showed no significant dependence on the numerical parameters if $h \leq \gamma/8$, $\tau \leq \gamma^3/16$. Moreover, mass lumping did not lead to significant differences in the numerical results when compared to approximations obtained with full quadrature.

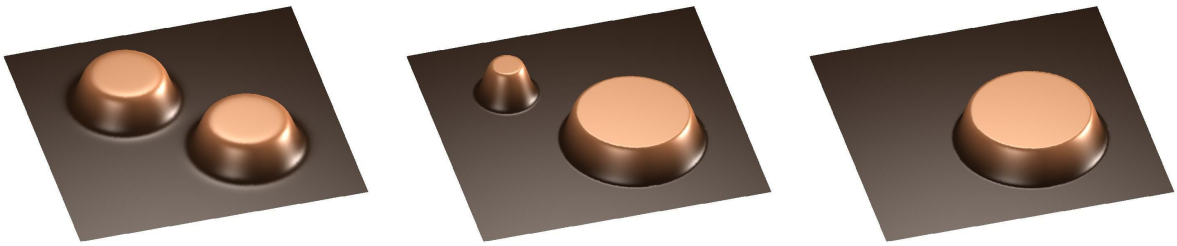

FIGURE 8. Absorption of a particle: snapshots of the solution from a simulation with $\theta = 0.2$ and $\gamma = 1/32$ at time $t = 0$, $t = 0.027$ and $t = 0.33$.

6.2.2. *Absorption of a particle.* We prescribe initial values representing two circular particles where one is slightly larger than the other. Figure 8 shows snapshots of the solution for $\theta = 0.2$ and $\gamma = 1/32$. Let $\Omega := (-1,1)^2$, $m_1 := (-1,1)/3$, $m_2 := (1,-1)/3$, $r_1 := 1/6$, $r_2 := 0.94\, r_1$ and define $d_j(x) := |x - m_j| - r_j$ for $x \in \Omega$ and $j = 1,2$. For given $\gamma > 0$ and $x \in \Omega$ let $u_0(x) := \max\left\{-u_{\mathrm{bi}}^{\theta}, \min\{\tilde{u}_0, u_{\mathrm{bi}}^{\theta}\}\right\}$ with

$$\tilde{u}_0(x) := -\tanh\left(\frac{d(x)}{\sqrt{2}\gamma}\right), \qquad d(x) := \max\{d_1(x), d_2(x)\}. \tag{17}$$

For $\theta = 0.2$, the time evolution of $\Lambda_{CH}(t)$ is plotted in Figure 9 for $\gamma = 1/16, 1/24, 1/32, 1/48$. We observe a peak at the time where the smaller particle vanishes but for $\gamma \to 0$ the quantity $\widetilde{E}$ according to (14) grows only less than $\gamma^{-3/2}$, see Figure 9. Different values of θ and the smooth quartic potential lead to the same qualitative results. Therefore, we conclude that robust error control past topological changes is possible.

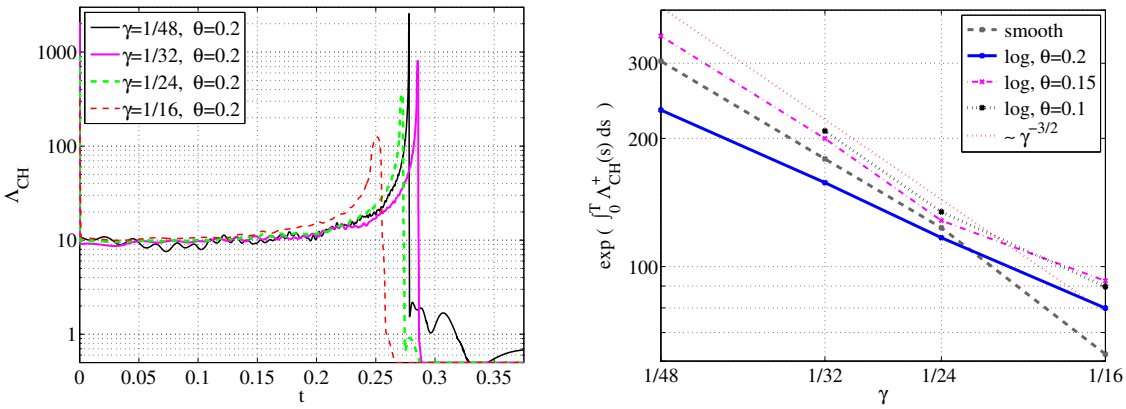

FIGURE 9. Numerically computed eigenvalue $\Lambda_{CH}(t)$ for $\theta = 0.2$ in the absorbtion of a particle: the peak indicates the time when the smaller particle vanishes (left). Robust error control past topological changes is possible since $\widetilde{E} \sim \gamma^{-3/2}$ (right).

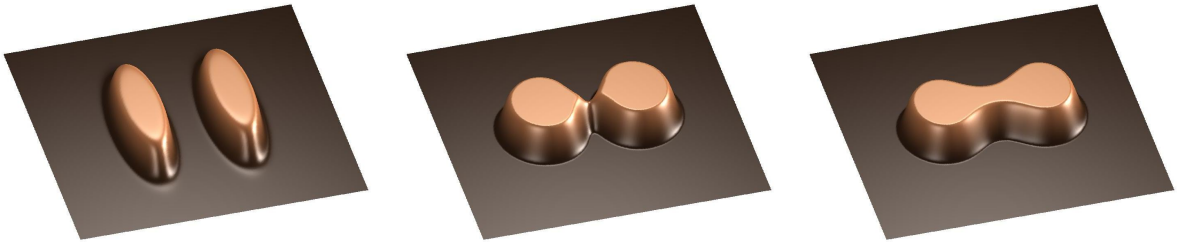

FIGURE 10. Merging of particles: snapshots of the solution from a simulation with $\theta = 0.2$ and $\gamma = 1/32$ at time $t = 0$, $t = 0.012$ and $t = 0.03$.

6.2.3. *Merging of particles.* We prescribe initial values representing two ellipsoidal particles such that the longer axes are parallel to each other, see Figure 10. Similar to the mean curvature motion of interfaces, the particles develop more and more circular shapes and thereby they come closer to each other until eventually they merge. After this topological change the merged particle evolves smoothly to a stable circular shape. Let $\Omega := (-1,1)^2$, $m_{1/2} := \pm(1/4+2\gamma, 0)$, $R := 1/6$ and define $d_j(x) := \left|\operatorname{diag}\left((1,1/3)(x-m_j)\right|\right. - R$ for $x \in \Omega$ and $j = 1,2$. For given $\gamma > 0$ and $x \in \Omega$ let $u_0(x) := \max\left\{-u^\theta_{\mathrm{bi}}, \min\{\tilde{u}_0, u^\theta_{\mathrm{bi}}\}\right\}$ with

$$\tilde{u}_0(x) := -\tanh\left(\frac{\sqrt{2}\,d(x)}{\gamma}\right), \qquad d(x) := \max\{d_1(x), d_2(x)\}. \tag{18}$$

In Figure 11, the time evolution of $\Lambda_{CH}(t)$ is plotted for $\theta = 0.2$ and $\gamma = 1/16, 1/24, 1/32, 1/48$. We observe a peak at the time where the particles merge but for $\gamma \to 0$ the quantity $\widetilde{E}$ according to (14) grows only like γ^{-2}, see Figure 11. Simulations with different values of θ and with the smooth quartic potential lead to the same qualitative results. Therefore, we conclude that robust error control past topological changes is possible.

6.2.4. *Allen–Cahn equation with logarithmic potential.* Let u_0 be given by (15) representing interfaces given by concentric circles. Instead of the Cahn–Hilliard evolution of Section 6.2.1 we now consider the Allen–Cahn evolution of diffuse interfaces. Because the Allen–Cahn equation is not mass conserving, we observe that after the inner surface disappeared the remaining particle shrinks until it also vanishes. This leads to two separate peaks in the eigenvalue $\Lambda_{AC}(t)$, see Figure 12.

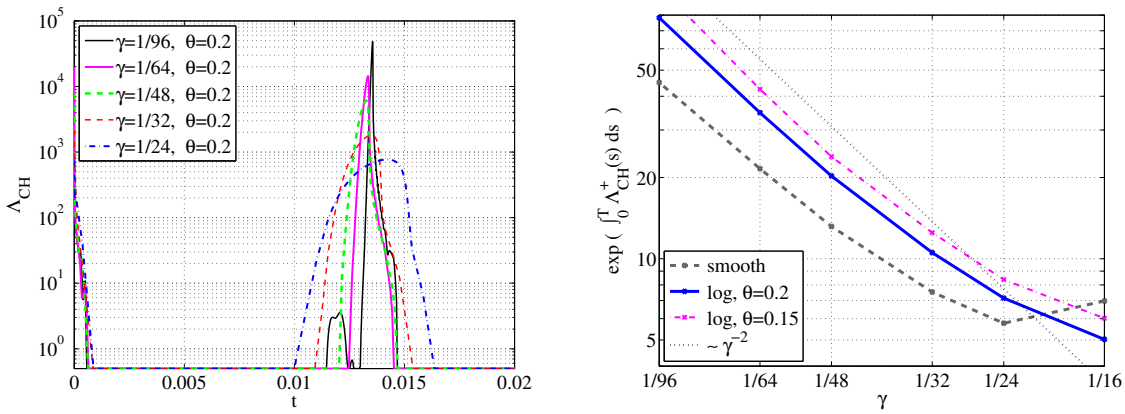

FIGURE 11. Numerically computed eigenvalue $\Lambda_{CH}(t)$ for $\theta = 0.2$ in the merging of two particles (left). Robust error control past topological changes is possible since $\widetilde{E}$ grows polynomially with respect to γ^{-1} (right).

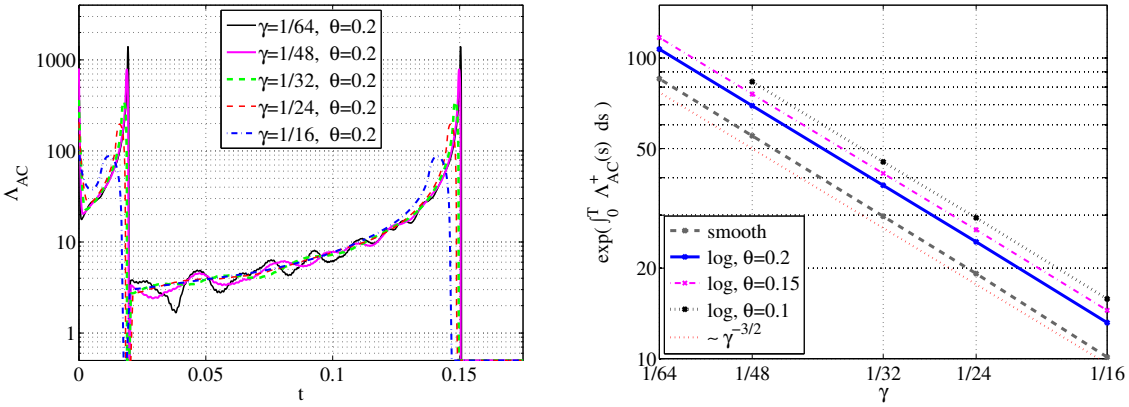

FIGURE 12. Allen–Cahn equation with two concentric circles on the initial profile: numerically computed eigenvalue $\Lambda_{AC}(t)$ for $\theta = 0.2$ (left). Robust error control past topological changes is possible since growth of $\widetilde{E}$ is only of order $\gamma^{-3/2}$ (right).

From the relation $\widetilde{E} \sim \gamma^{-3/2}$ in Figure 12, we conclude that robust error control past topological changes is possible. For smooth potentials, a similar behavior was reported in [BMO09].

6.3. **Dependence on temperature and the limit $\theta \to 0$.** When θ becomes small, the binodal point u^θ_{bi} gets transcendentally close to the singular point. This causes both theoretical as well as practical problems. Numerical calculations must break down, if the distance $1 - u^\theta_{\mathrm{bi}}$ is below floating point accuracy. Already before that, the iterative solution of the nonlinear system within each time step becomes more expensive as θ decreases. When all other parameters are kept fixed, the graphs of $\Lambda_{AC}(t)$ or $\Lambda_{CH}(t)$ show oscillations that increase as $\theta \to 0$ although the amplitudes of the oscillations are still several orders of magnitude smaller than the peaks of the computed eigenvalues.

The smallness condition in Proposition 3.2 and 4.4 involves the number B that depends on $\theta \|\phi'''(u_1(s))\|_{L^\infty(\Omega)}$. For the potential (2) we have $\phi'''(u) \sim u/(1-u^2)$. Since $1 - u^\theta_{\mathrm{bi}}$ decreases exponentially for $\theta \to 0$ and the solution may attain values arbitrarily close to the binodal points, B may grow faster than polynomially. To show robustness of the error estimates for small θ would

therefore require a refined analysis. Nevertheless, the previous numerical experiments indicate that the quantities $\widetilde{E}$ and hence E converge for $\theta \to 0$, see Figure 6, 9, 11 and 12.

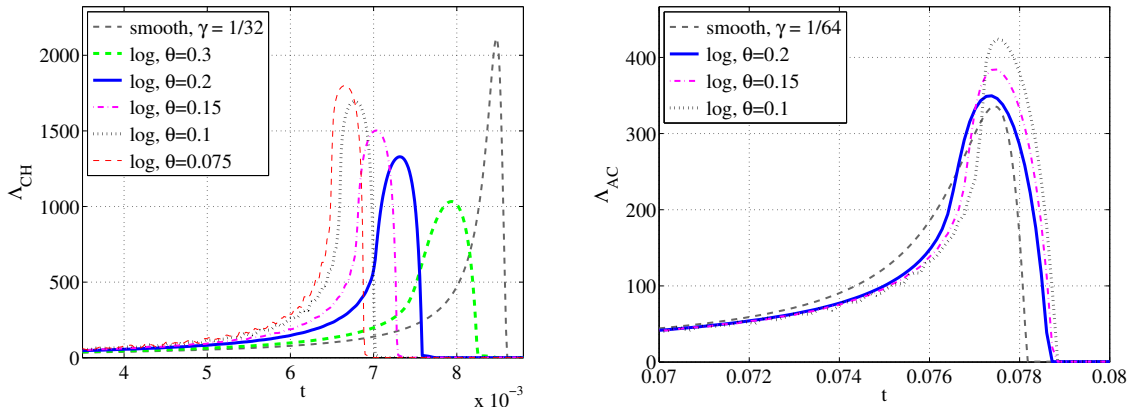

FIGURE 13. Zoom of the principal eigenvalues from Section 6.2.1 and 6.2.4 with a linear scaling on the y-axis: for fixed γ, the graphs of $\Lambda_{CH}(t)$ (left) and $\Lambda_{AC}(t)$ (right) converge as $\theta \to 0$.

In the limiting problem with the double obstacle potential, it is not obvious how to formulate the correct linearization and the corresponding eigenvalue problem. But the results of the previous numerical experiments allow a meaningful extrapolation for $\theta = 0$. Figure 13 shows for different θ the time evolution of the principal eigenvalue during a topological change in the solution. In the Cahn–Hilliard case from Section 6.2.1, we observe that for decreasing θ, the topological change occurs earlier. The position, height and the width of the peak in $\Lambda_{CH}(t)$ show an affine dependence on θ. The numerical experiments in Section 6.2.2 and 6.2.3 confirm all these relations. In contrast, for the principal eigenvalue $\Lambda_{AC}(t)$ in the Allen–Cahn case of Section 6.2.4, we observe that the position of the peak has a much weaker dependence on the potential but for decreasing θ the topological change now occurs slightly later. Again, the height of the peak in $\Lambda_{AC}(t)$ depends on θ in an affine way whereas the width seems independent of θ.

Acknowledgments. S.B. acknowledges support by the DFG through the Collaborative Research Center (SFB) 611 *Singular Phenomena and Scaling in Mathematical Models.*

REFERENCES

[ABC94] N. Alikakos, P. Bates, and X. Chen. Convergence of the Cahn–Hilliard equation to the Hele-Shaw model. *Arch. Rat. Mech. Anal.*, 128:165–205, 1994.

[AC79] S. Allen and J. W. Cahn. A microscopic theory for antiphase boundary motion and its application to antiphase domain coarsening. *Acta. Metall.*, 27:1084–1095, 1979.

[Bar05] S. Bartels. A posteriori error analysis for time-dependent Ginzburg–Landau type equations. *Numer. Math.*, 99(4):557–583, 2005.

[Bar10] S. Bartels. A lower bound for the spectrum of the linearized Allen–Cahn operator near a singularity. Preprint available at `www.bartels.ins.uni-bonn.de`, 2010.

[BB95] J. W. Barrett and J. F. Blowey. An error bound for the finite element approximation of the Cahn–Hilliard equation with logarithmic free energy. *Numer. Math.*, 72(1):1–20, 1995.

[BB99] J. W. Barrett and J. F. Blowey. Finite element approximation of the Cahn–Hilliard equation with concentration dependent mobility. *Math. Comp.*, 68(226):487–517, 1999.

[BBG99] J. W. Barrett, J. F. Blowey, and H. Garcke. Finite element approximation of the Cahn–Hilliard equation with degenerate mobility. *SIAM J. Numer. Anal.*, 37(1):286–318 (electronic), 1999.

[BE91] J. F. Blowey and C. M. Elliott. The Cahn–Hilliard gradient theory for phase separation with nonsmooth free energy. I. Mathematical analysis. *European J. Appl. Math.*, 2(3):233–280, 1991.

[BE92] J. F. Blowey and C. M. Elliott. The Cahn–Hilliard gradient theory for phase separation with nonsmooth free energy. II. Numerical analysis. *European J. Appl. Math.*, 3(2):147–179, 1992.

[BM10a] S. Bartels and R. Müller. A posteriori error controlled local resolution of evolving interfaces for generalized Cahn–Hilliard equations. *Interfaces Free Bound.*, 12(1):45–73, 2010.

[BM10b] S. Bartels and R. Müller. Quasi-optimal and robust a posteriori error estimates in $L^\infty(L^2)$ for the approximation of Allen–Cahn equations past singularities. Preprint available at `www.bartels.ins.uni-bonn.de`, 2010.

[BMO09] S. Bartels, R. Müller, and C. Ortner. Robust a priori and a posteriori error analysis for the approximation of Allen–Cahn and Ginzburg–Landau equations past topological changes. Preprint available at `www.bartels.ins.uni-bonn.de`, 2009.

[BN09] L. Baňas and R. Nürnberg. A posteriori estimates for the Cahn–Hilliard equation with obstacle free energy. *M2AN Math. Model. Numer. Anal.*, 43(5):1003–1026, 2009.

[Cah61] J. W. Cahn. On spinodal decomposition. *Acta. Metall.*, 9:795–801, 1961.

[CE92] M. I. M. Copetti and C. M. Elliott. Numerical analysis of the Cahn–Hilliard equation with a logarithmic free energy. *Numer. Math.*, 63(1):39–65, 1992.

[CH58] J. W. Cahn and J. E. Hilliard. Free energy of a non-uniform system. I. interfacial free energy. *J. Chem. Phys.*, 28:258–267, 1958.

[Che94] X. Chen. Spectrum for the Allen–Cahn, Cahn–Hilliard, and phase-field equations for generic interfaces. *Commun. Partial Diff. Eqs.*, 19(8):1371–1395, 1994.

[CM95] L. A. Caffarelli and N. E. Muler. An L^∞ bound for solutions of the Cahn–Hilliard equation. *Arch. Rational Mech. Anal.*, 133(2):129–144, 1995.

[dMS95] P. de Mottoni and M. Schatzman. Geometrical evolution of developed interfaces. *Trans. Amer. Math. Soc.*, 347:1533–1589, 1995.

[EG96] C. M. Elliott and H. Garcke. On the Cahn–Hilliard equation with degenerate mobility. *SIAM J. Math. Anal.*, 27(2):404–423, 1996.

[ES86] C. M. Elliott and Z. Songmu. On the Cahn–Hilliard equation. *Arch. Rational Mech. Anal.*, 96(4):339–357, 1986.

[FP03] X. Feng and A. Prohl. Numerical analysis of the Allen–Cahn equation and approximation for mean curvature flows. *Numer. Math.*, 94(1):33–65, 2003.

[FP04] X. Feng and A. Prohl. Error analysis of a mixed finite element method for the Cahn–Hilliard equation. *Numer. Math.*, 99(1):47–84, 2004.

[FW08] X. Feng and H. Wu. A posteriori error estimates for finite element approximations of the Cahn–Hilliard equation and the Hele-Shaw flow. *J. Comput. Math.*, 26(6):767–796, 2008.

[KNS04] D. Kessler, R. H. Nochetto, and A. Schmidt. A posteriori error control for the Allen–Cahn problem: circumventing Gronwall's inequality. *M2AN Math. Model. Numer. Anal.*, 38(1):129–142, 2004.

[LM06] O. Lakkis and C. Makridakis. Elliptic reconstruction and a posteriori error estimates for fully discrete linear parabolic problems. *Math. Comp.*, 75(256):1627–1658 (electronic), 2006.

[LU68] O.A. Ladyzhenskaya and N.N. Ural'tseva. *Linear and quasilinear elliptic equations.* Translated from the Russian by Scripta Technica, Inc. Translation editor: Leon Ehrenpreis. Academic Press, New York, 1968.

[MN03] C. Makridakis and R. H. Nochetto. Elliptic reconstruction and a posteriori error estimates for parabolic problems. *SIAM J. Numer. Anal.*, 41(4):1585–1594 (electronic), 2003.

[NV97] R. H. Nochetto and C. Verdi. Convergence past singularities for a fully discrete approximation of curvature-driven interfaces. *SIAM J. Numer. Anal.*, 34(2):490–512, 1997.

[PF90] O. Penrose and P. C. Fife. Thermodynamically consistent models of phase-field type for the kinetics of phase transitions. *Phys. D*, 43(1):44–62, 1990.